Journal of Power Sources 196 (2011) 9751–9756

Contents lists available at ScienceDirect

Journal of Power Sources

journal homepage: www.elsevier.com/locate/jpowsour

In situ ceramic fillers of electrospun thermoplastic polyurethane/poly(vinylidene fluoride) based gel polymer electrolytes for Li-ion batteries

Na Wu, Qi Cao*, Xianyou Wang, Sheng Li, Xiaoyun Li, Huayang Deng

Key Laboratory of Environmentally Friendly Chemistry and Applications of Minister of Education, College of Chemistry, Xiangtan University, Xiangtan 411105, China

ARTICLE INFO

Article history:
Received 31 May 2011
Received in revised form 21 July 2011
Accepted 22 July 2011
Available online 29 July 2011

Keywords:
Gel polymer electrolyte
Electrospinning
In situ ceramic fillers
Thermoplastic polyurethane
Poly(vinylidene fluoride)

ABSTRACT

Gel polymer electrolyte films based on thermoplastic polyurethane (TPU)/poly(vinylidene fluoride) (PVdF) with and without in situ ceramic fillers (SiO_2 and TiO_2) are prepared by electrospinning 9 wt% polymer solution at room temperature. The electrospun TPU–PVdF blending membrane with 3% in situ TiO_2 shows a highest ionic conductivity of 4.8×10^{-3} S cm^{-1} with electrochemical stability up to 5.4 V versus Li^+/Li at room temperature and has a high tensile strength (8.7 ± 0.3 MPa) and % elongation at break (110.3 ± 0.2). With the superior electrochemical and mechanical performance, it is very suitable for application in polymer lithium ion batteries.

1. Introduction

Gel polymer electrolyte (GPE) has attracted much attention of the researchers. They aim at developing novel GPE with both higher ionic conductivity and good mechanical properties. Many methods for preparing GPE have been tried to improve the ionic conductivity, such as phase inversion method, γ-ray irradiation method, solvent casting technique, TIPS technique, and electrospinning technique [1,2]. Among these methods, electrospinning technique is a very unique and useful way to prepare GPE with superior performance [3–5]. Furthermore the choice of matrices for GPE is also very important. And a lot of work has been done [6–13]. Thermoplastic polyurethane (TPU) belongs to an elastomer class possessing high tensile strength, elasticity as well as low crystallinity. TPU has two-phase microstructure: the soft segments and the hard segments. The hard and soft phases are thermodynamically incompatible, which promotes hydrogen bonding within the hard domain involving urethane C=O and N–H moieties on adjacent polymer chain segments. The hard segments are interconnected throughout the soft phase parts, and play the role of keeping dimensional stability. While the soft segments dissolve alkali metal without formation of ionic cluster and offer the whole system with good ionic conductivity. Poly(vinylidene fluoride) (PVdF) is a semicrystalline polymer. With high mechanical and anodically stability, PVdF has been adopted as polymer electrolytes in lithium batteries. Moreover doping ceramic fillers, such as TiO_2, SnO_2, MgO, Al_2O_3, and SiO_2, is an effective way to improve the electrochemical and mechanical properties of GPE [4,14–18].

In this work, we choose thermoplastic polyurethane (TPU)/poly(vinylidene fluoride) (PVdF) as electrospun matrix, which has very significant enhancement on mechanical properties. Therefore, TPU–PVdF based gel polymer electrolyte with and without in situ ceramic fillers (SiO_2 and TiO_2) are prepared by electrospinning technique. The properties of electrospun membranes prepared with in situ ceramic fillers (SiO_2 and TiO_2) are observed to be comparatively better than the one prepared without in situ ceramic fillers. And the electrospun TPU–PVdF blending membrane with 3% in situ TiO_2 has the most superior performance.

2. Experimental

2.1. Materials

Thermoplastic polyurethane (TPU, yantaiwanhua, 1190A) and Poly(vinylidene fluoride) (PVdF, Alfa Aesar) were dried under vacuum at 80 °C for 24 h. $LiClO_4 \cdot 3H_2O$ (AR, Sinopharm Chemical Reagent Co., Ltd.) was dehydrated in vacuum oven at 120 °C for 72 h. 1.0 M Liquid electrolyte was made by dissolving a certain quality of $LiClO_4$ in ethylene carbonate (EC, Shenzhen Capchem Technology Co., Ltd.)/propylene carbonate (PC, Shenzhen Capchem Technology Co., Ltd.) (1/1, v/v), tetraethoxy silane (TEOS, Aldrich), tetrabutyl titanate (TBT, Aldrich), ammonium hydroxide (25% NH_3 in water, Daejung Chem), acetic acid glacial (CH_3COOH, AR),

* Corresponding author. Tel.: +86 731 58298090; fax: +86 731 58298090.
E-mail address: wjcaoqi@163.com (Q. Cao).

0378-7753/$ – see front matter © 2011 Elsevier B.V. All rights reserved.
doi:10.1016/j.jpowsour.2011.07.079

N,N-dimethylforamide (DMF) and acetone were analytical purity and used as received without further treatment.

2.2. Preparation of TPU–PVdF fibrous membrane

Three types of TPU–PVdF fibrous membranes (a) without in situ ceramic fillers, (b) with 3% in situ SiO_2 and (c) with 3% in situ TiO_2 were prepared by electrospinning the following solutions, respectively.

(a) A 9% solution of TPU–PVdF (1:1, w/w) in DMF/acetone (3:1, w/w) was prepared by magnetic stirring for 12 h at room temperature.

(b) A 9% solution of TPU–PVdF (1:1, w/w) in DMF/acetone (3:1, w/w) was prepared by magnetic stirring for 12 h at room temperature. For generating in situ SiO_2, a small quantity of ammonium hydroxide (3–4 drops) was added to the polymer solution, which was followed by drop wise addition of the required quantity of TEOS under vigorous stirring. The stirring was continued at room temperature until forming a homogeneous solution.

The hydrolysis and condensation reactions of TEOS can be represented by the following equations:

$$Si(OC_2H_5)_4 + 4H_2O \rightarrow Si(OH)_4 + 4C_2H_5OH\,(\text{hydrolysis})$$

$$Si(OH)_4 \rightarrow SiO_2(s) + 2H_2O\,(\text{condensation})$$

(c) Firstly a 9% TPU–PVdF (1:1, w/w)/DMF/acetone (3:1, w/w) solution was also prepared following the step (b). For generating in situ TiO_2, a small quantity of acetic acid glacial (3–4 drops) and the required quantity of TBT were added to the polymer solution under vigorous stirring. The stirring was continued at room temperature until forming a homogeneous solution.

The hydrolysis and condensation reactions of TBT can be represented by the following equations:

$$Ti(OC_2H_5)_4 + 4H_2O \rightarrow Ti(OH)_4 + 4C_2H_5OH\,(\text{hydrolysis})$$

$$n\,Ti(OH)_4 \rightarrow TiO_2(s) + 2nH_2O\,(\text{condensation})$$

All of the solutions were electrospun under high voltage of 28.5 kV at room temperature, respectively. Nonwoven films were obtained on the collector plate and put on the table overnight to ensure the hydrolysis and condensation reactions fully completed. Then the electrospun nonwoven films were dried under vacuum at 80 °C for 12 h.

2.3. Preparation of gel polymer electrolytes

The thickness of the electrospun nonwoven films used were ~100 μm. At room temperature, the dried electrospun nonwoven films were activated by dipping in 1 M $LiClO_4$–EC/PC liquid electrolyte solutions for 1 h in a glove box filled with argon. Wipe the surface of swelled membranes by filter paper and then get gel polymer electrolytes.

2.4. Membrane characterization

The morphology of films was examined by Scanning electron microscope (SEM, Hitachi S-3500N, Japan). The structure was investigated by FTIR spectra (Spectrum One, PerkinElmer Instruments).

The thermal characterization of the prepared polymer networks was carried out by Differential Scanning Calorimeter (DSC) with a heating and cooling rate of 20 °C min^{-1} on a DSC TA (DSC-7, PerkinElmer Co., USA) instrument. Samples were run under a nitrogen atmosphere over a temperature range of −90 to 230 °C. The crystallinity (χ_c) was calculated based on the following Eq. (A) from the DSC curves.

$$\chi_c = \frac{\Delta H_f}{\Delta H_f^* \phi} \times 100\% \quad (A)$$

where ΔH_f and ΔH_f^* represent the fusion enthalpy of blend membrane and PVdF with 100% crystallinity, respectively. The value of ΔH_f^* is 104.7 J g^{-1}. ϕ is the measuring weight fraction of PVdF.

The mechanical strength of the polymer gel electrolyte films was measured by universal testing machines (UTM, Instron Instruments). The extension rate was kept at ~10 mm min^{-1}. The dimensions of the sheet used were ~2 cm × 5 cm × ~150–250 μm (width × length × thickness).

The porosity was investigated by immersing the membranes into *n*-butanol for 1 h and then calculated by using the following relation: $P = (W_w - W_d/\rho_b V_p) \times 100\%$, where W_w and W_d are the mass of the wet and dry membrane, respectively, ρ_b the density of *n*-butanol, and V_p the volume of the dry membrane.

The electrolyte uptake was determined by measuring the weight increase and calculated according to the following Eq. (B):

$$\text{Uptake}\,(\%) = \frac{W - W_0}{W_0} \times 100 \quad (B)$$

where W_0 is the weight of dried films and W is the weight of swelled films.

The ionic conductivity of the composite film was measured with SS/PE/SS blocking cell by AC impedance measurement using Zahner Zennium electrochemical analyzer with a frequency range of 0.1–1 MHz. The thin films were prepared about 100 μm in thickness and 2.24 cm^2 in area for impedance measurement. Thus, the ionic conductivity could be calculated from the following Eq. (C):

$$\sigma = \frac{h}{RbS} \quad (C)$$

In this equation, σ is the ionic conductivity, Rb is the bulk resistance, h and S is the thickness and area of the films, respectively.

Electrochemical stability was measured by a linear sweep voltammetry (LSV) of a Li/PE/SS cell using Zahner Zennium electrochemical analyzer at a scan rate of 5 mV s^{-1}, with voltage from 2.5 V to 6 V.

3. Results and discussion

3.1. Morphology and structure

Fig. 1 shows the SEM images of the membranes prepared by electrospinning of polymer solution with and without in situ ceramic fillers. All of the fibers mentioned above appear to be uniform in composition without having any microphase separation which due to the miscibility of TPU and PVdF. It is well known that TPU is a linear polymer material and the molecular structure is complicated. The duplicated carbamated-chain (–R′–O–CO–NH–R–NH–CO–O–), which is in the hard segments of TPU, offers amino-group (–NH). The amino-group (–NH) can form hydrogen bonds with the strong electron-withdrawing functional group (–C–F) which is in the backbone structure of PVdF. Therefore, PVdF and TPU are miscible without any microphase separation as electrospun matrix.

A network of interlaid and nearly straightened tubular structure fibers are found in the membrane without in situ ceramic fillers (Fig. 1(a)) and the average fiber diameter (AFD) is about ~0.57 μm. As shown in Fig. 1(b), there are many beads in the fiber membrane which dues to a lower dispersion of the SiO_2 nano-particles and the AFDs of the membrane with in situ SiO_2 are about 0.43 μm. While the membrane with in situ TiO_2 in Fig. 1(c) has interconnected multifibrous layers with ultrafine porous structure and a lowest AFD of about ~0.30 μm. The morphology of in situ TiO_2 sample seems to

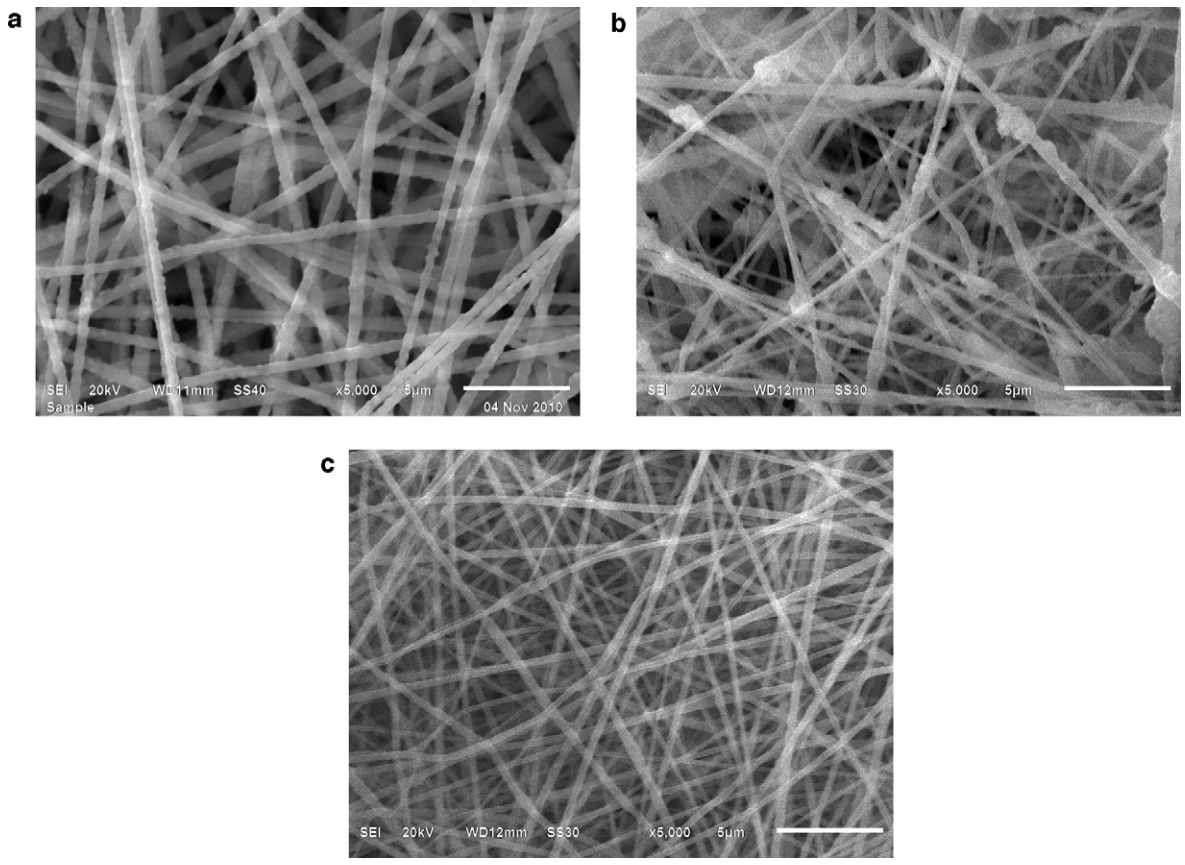

Fig. 1. SEM images of electrospun TPU–PVdF membranes (a) without in situ ceramic fillers, (b) with 3% in situ SiO_2 and (c) with 3% in situ TiO_2.

be the same as that of pristine membrane, indicating that nano TiO_2 particles are homogeneously dispersed in the polymeric matrix.

As described in TPU–PVdF fibrous membrane preparation steps, the hydrolysis and condensation reactions took place for generating in situ ceramic fillers (SiO_2 and TiO_2). The present method of preparation is able to produce and maintain a high dispersion of the inorganic phase in the polymer matrix. The viscous of polymer solution and the steric hindrance reduced the movement of hydrolyzed precursor molecules. So the probability of the resulting sol nuclei meeting one another to grow into an extended structure or large particles is greatly reduced. Under this condition, only a limited amount of sol particles are able to undergo gelation to form large assemblies, and most ceramic fillers exists as isolated nanoscale particles.

Following the hydrolyzed precursor molecules added, the viscosity of polymer solution is lower than the pristine solution. This is the main reason for the formation of finer fibers. So the AFDs of the membrane with in situ ceramic fillers are lower than the pristine membrane. The lower AFD is, the higher electrolyte uptake is [19,20]. This predicts the membrane with in situ TiO_2 will have a highest ionic conductivity.

FT-IR spectra of the composite membrane with and without in situ ceramic fillers are shown in Fig. 2. In Fig. 2(a), the characteristic absorption peaks of TPU (3308 cm^{-1} and 1727 cm^{-1}) and PVdF (1399 cm^{-1}, 1073 cm^{-1} and 877 cm^{-1}) are present clearly, indicating that the blend membrane consists of two compounds: TPU and PVdF. And the strong electron-withdrawing functional group (–C–F) which is in the backbone structure of PVdF can form hydrogen bonds with amino-group (–NH) which is in the hard segments of TPU duing to a little shift of absorption bands (1403 cm^{-1}, 1075 cm^{-1} and 876 cm^{-1}) in the characteristic absorption peaks of the TPU/PVdF based membrane.

The vibration peak at 1507 cm^{-1} in Fig. 2(c) perhaps belongs to the TiO_2. The intensity of the absorption peaks at 1403, 1075, and 876 cm^{-1} of the TPU/PVdF membrane with in situ TiO_2 decrease due to the interactions between the nanoparticles and the polymer chains suggesting that the polarity of the CF_2 groups decreases. In the spectrum of the membrane with in situ SiO_2 (Fig. 2(b)), the integral area of the wide peak at around 1110 cm^{-1} increases because the absorption peak of the Si–O–Si band of SiO_2 is at around 1110 cm^{-1}.

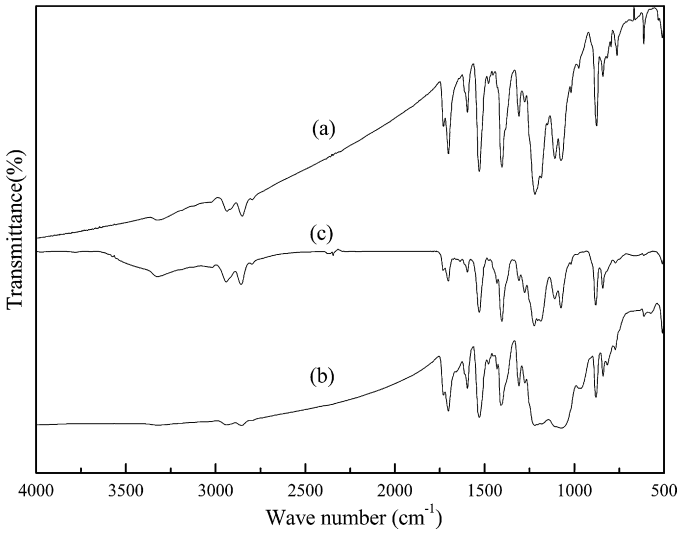

Fig. 2. FTIR spectra of the electrospun TPU–PVdF membranes (a) without in situ ceramic fillers, (b) with 3% in situ SiO_2 and (c) with 3% in situ TiO_2.

Table 1
Crystallinity (χ_c), porosity and mechanical properties of TPU–PVdF fibrous membranes (a) without in situ ceramic fillers, (b) with 3% in situ SiO_2 and (c) with 3% in situ TiO_2.

Sample name	Surface area (cm^2)	Porosity (%)	ΔH_f ($J\,g^{-1}$)	χ_c (%)	Tensile strength (MPa)	Elongation at break (%)
TPU/PVdF	2.716	86	20.65	39.45	6.8 ± 0.2	85.8 ± 0.2
TPU/PVdF/SiO_2(3%)	2.583	89	11.16	21.32	9.7 ± 0.1	91.9 ± 0.1
TPU/PVdF/TiO_2(3%)	2.349	96	7.464	14.26	8.7 ± 0.3	110.3 ± 0.2

3.2. DSC analysis and mechanical properties

Fig. 3 displays DSC curves and the following observations were made. As shown in Fig. 3, the melting temperature of the eletrospun membrane without in situ ceramic fillers ((a) in Fig. 3) is 101.1 °C, while the membranes with in situ ceramic fillers (SiO_2 and TiO_2) ((b) and (c) in Fig. 3) have lower melting temperatures in the range of 100.1–100.7 °C. Although the melting temperatures are nearly the same, the melting enthalpy (ΔH_f) of the membrane with in situ ceramic fillers (SiO_2 and TiO_2) is much lower than that of the membrane without in situ ceramic fillers. As shown in Table 1, the ΔH_f of membrane without in situ ceramic fillers is 20.65 $J\,g^{-1}$, while the membrane with in situ ceramic fillers is 11.16 $J\,g^{-1}$ (in situ SiO_2) and 7.464 $J\,g^{-1}$ (in situ TiO_2), respectively. According to Eq. (A), the percentage of crystallinity values obtained from the DSC data follows the order: in situ TiO_2 (14.26%) < in situ SiO_2 (21.32%) < membrane without in situ ceramic fillers (39.45%). The reduction in crystallinity may result from the partial inhibition effect of SiO_2 and TiO_2 addition on polymer crystal formation, just as the inorganic fillers such as α-Al_2O_3, TiO_2, SiO_2, $BaTiO_3$ decreased the crystalline phase of polymer electrolyte system [21–23]. The formation of lewis acid–base interactions between the nano-sized ceramic fillers and polar groups of the polymer chains inhibits the crystallization process of the polymer. It increases the amorphous regions in the polymer. Lower crystallinity of membrane can supply a beneficial condition for higher conductivity enhancement. The results suggested that the membrane with in situ TiO_2 may have the excellent ionic conductivity.

Fig. 4 shows the stress–strain curves of the polymer membranes. And the mechanical test dates of the membranes are also given in Table 1. The results of mechanical strength test show that the in situ ceramic fillers improved the mechanical performance of membranes. Both the tensile strength and elongation at break were enhanced. The reasons are as below. Nano-particle has small size and large surface area. Thus it has a great contact area with the polymeric matrix. When the material is struck, the more microcracking will absorb more impact energy. So the further expansion of the cracks is blocked.

Elongation at break often reflects the impact performance of material and the impact resistance is shown by the material toughness. The higher toughness in mechanical properties will reduce the risk of the collapse of the membrane, which is suggests that the membrane with in situ ceramic fillers is more suitable for application in polymer lithium ion batteries.

3.3. Porosity and electrolyte uptake

The results of porosity of the membranes are given in Table 1. As shown, all of the membranes had good porosity due to their well-developed interstices by the interwoven structure among nanofibers. A porosity of 96% was found for the membrane with in situ TiO_2, while it was higher than the membrane with in situ SiO_2 (89%) and the membrane without in situ ceramic fillers (86%).

The difference in porosity is attributed to the three-dimensional structure of the membranes. From the results of SEM, we can find that the membrane with in situ TiO_2 has the lowest AFDs. The AFD significantly affected the physical properties of the fibrous membranes such as their porosity, pore size, pore size distribution and specific surface area, and so on. In the certain volume, the pores, which are formed by fiber overlapping, will increase when the average fiber diameters decrease. So the membrane with in situ TiO_2 shows the highest porosity.

Fig. 5 shows the uptake behavior of the electrospun TPU–PVdF fibrous membranes. The percentage of electrolyte uptake can be calculated according to Eq. (B). The fibrous film without in situ ceramic fillers (Fig. 5(a)) shows an electrolyte uptake of about 312% within 2 min, while the membrane with in situ SiO_2 (Fig. 5(b)) is 300% and the membrane with in situ TiO_2 (Fig. 5(c)) is 336%. The uptake of the electrolyte solution reaches up to 342% (the membrane without in situ ceramic fillers), 346% (the membrane with in situ SiO_2) and 372% (the membrane with in situ TiO_2),

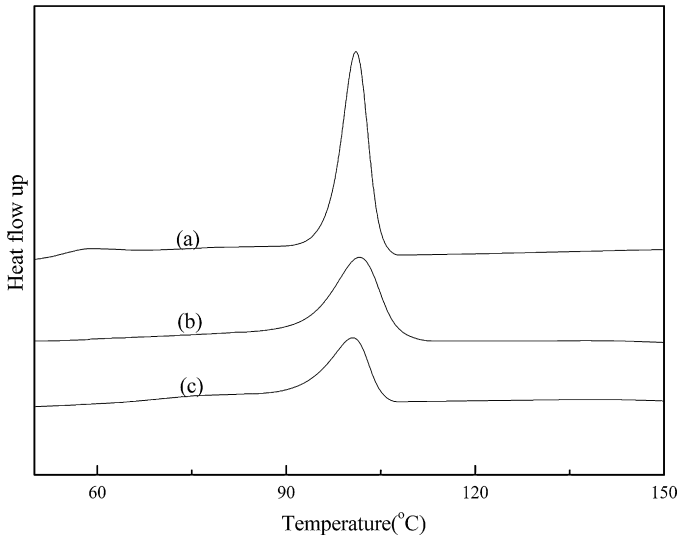

Fig. 3. DSC curves of TPU–PVdF fibrous membranes (a) without in situ ceramic fillers, (b) with 3% in situ SiO_2 and (c) with 3% in situ TiO_2.

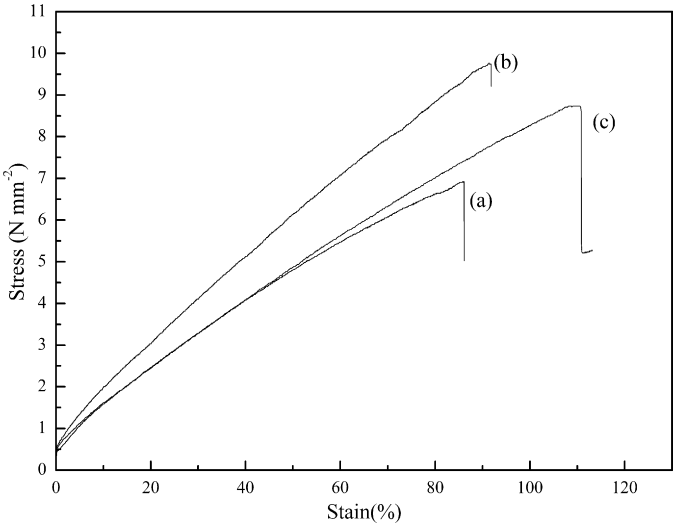

Fig. 4. Stress–strain curves of the electrospun TPU–PVdF membranes (a) without in situ ceramic fillers, (b) with 3% in situ SiO_2 and (c) with 3% in situ TiO_2.

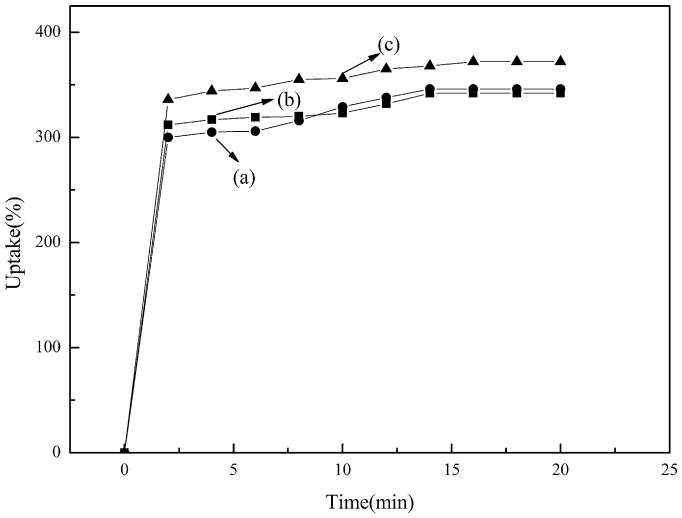

Fig. 5. The uptake behavior of the electrospun TPU–PVdF fibrous films (a) without in situ ceramic fillers, (b) with 3% in situ SiO_2 and (c) with 3% in situ TiO_2.

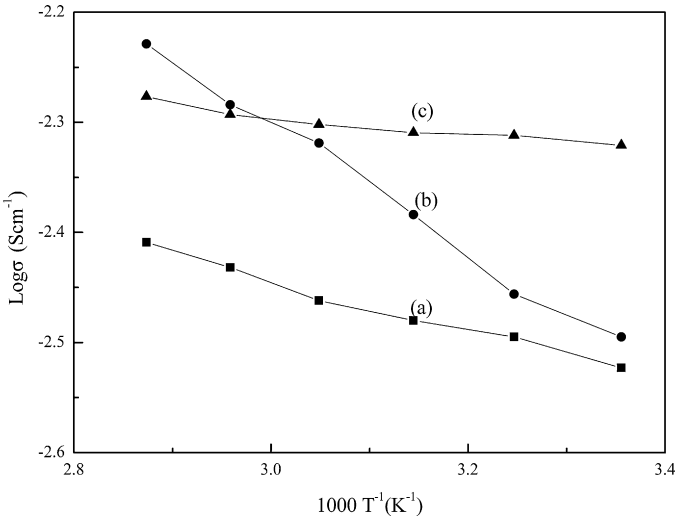

Fig. 7. The variation of ionic conductivity with temperature of the gel polymer electrolytes (a) without in situ ceramic fillers, (b) with 3% in situ SiO_2 and (c) with 3% in situ TiO_2.

respectively. After 15 min, it is found that when the electrolyte uptake of these three carves become stabile, the membrane with in situ TiO_2 always owns the highest electrolyte uptake percentage.

The absorption of large quantities of liquid electrolyte by the composite membranes results from the high porosity of the membranes and the high amorphous content of the polymer. The fully interconnected pore structure makes fast penetration of the liquid into the membrane possible, and hence the uptake process is stabile within the initial 15 min. The membrane with in situ TiO_2 owns the highest porosity, so it always has the highest electrolyte uptake percentage. This leads it to have a high ionic conductivity.

3.4. Ionic conductivity

Fig. 6 shows the impedance spectra of the gel polymer electrolytes with and without in situ ceramic fillers. It is a typical AC impedance for gel polymer electrolyte. It can be observed clearly from Fig. 6(a) that the bulk resistance (Rb) of the polymer electrolyte without in situ ceramic fillers is 1.4 Ω. And in Fig. 6(b) the electrolyte with in situ SiO_2 has a bulk resistance of 1.25 Ω. However, in Fig. 6(c) the bulk resistance (Rb) of the polymer electrolyte

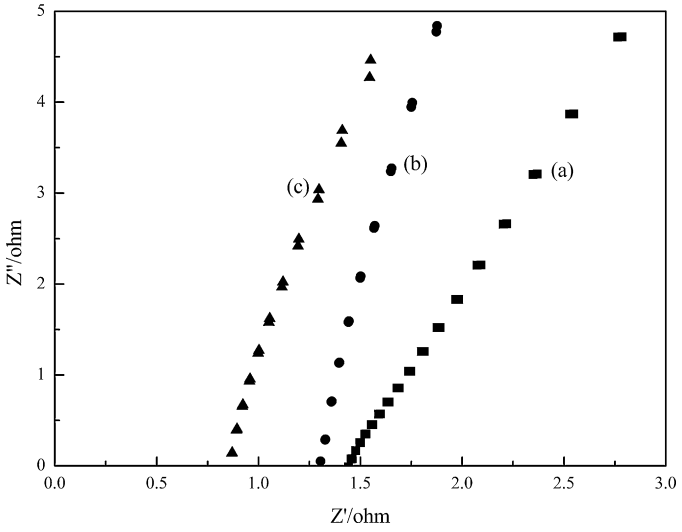

Fig. 6. Impedance spectra of the gel polymer electrolytes (a) without in situ ceramic fillers, (b) with 3% in situ SiO_2 and (c) with 3% in situ TiO_2.

with in situ TiO_2 is only 0.8 Ω. The ionic conductivity could be calculated with Eq. (C). The gel polymer electrolyte film has an ionic conductivity of 3.2×10^{-3} S cm^{-1} (GPE without in situ ceramic fillers), 3.8×10^{-3} S cm^{-1} (GPE with in situ SiO_2), 4.8×10^{-3} S cm^{-1} (GPE with in situ TiO_2), respectively.

Fig. 7 shows the temperature dependence of ionic conductivity of gel polymer electrolyte with and without in situ ceramic fillers (SiO_2 and TiO_2) in the range 25–75 °C. The conductive behavior obeys to Arrhenius equation $\sigma = \sigma_0 \exp(-E_a/RT)$, where R is the gas constant, σ is the conductivity of polymer electrolyte, σ_0 is the pre-exponential index and T is the testing absolute temperature.

The ionic conductivity of the gel polymer electrolyte without in situ ceramic fillers is 3.2×10^{-3} S cm^{-1} at 25 °C while those with in situ ceramic fillers are markedly increased. Compared with the gel electrolyte with in situ SiO_2, the ionic conductivity of the one with in situ TiO_2 is always higher and changes more stable as the temperature increasing. This is due to the slow ion conduction path in the swollen submicron fiber phase and the poor tortuosity in the pore structure. Also the ionic conductivity is dependent on the AFD or the porosity of the fibrous membranes. The ionic conductivity increased with the decrease in AFD, which resulted from the higher electrolyte uptake. Besides TiO_2 particles has a better dispersion and the in situ TiO_2 GPE system owns a better stabilization as a whole. So the GPE with in situ TiO_2 has the highest ionic conductivity and shows the most stable performance with the temperature changing.

One of the important reasons for the enhancement of conductivity for all in situ GPEs has been reported as the Lewis acid–base interactions between the filler particles and the electrolyte polar groups, and association between the filler particle and the polymer chains [21]. And the decreased polymer crystallinity in the presence of the inorganic particles is another important reason. In this study, the enhancement of conductivity is also attributed to these factors.

3.5. Electrochemical stability

The results of electrochemical stability tests of the gel polymer electrolytes by LSV are shown in Fig. 8. The electrochemical stability is at 4.8 V for the gel polymer electrolyte with pure liquid electrolyte (Fig. 8(a)). With the addition of the in situ ceramic fillers, the stability of the gel polymer electrolytes are further enhanced [24,25]. Their electrochemical stability follows the order:

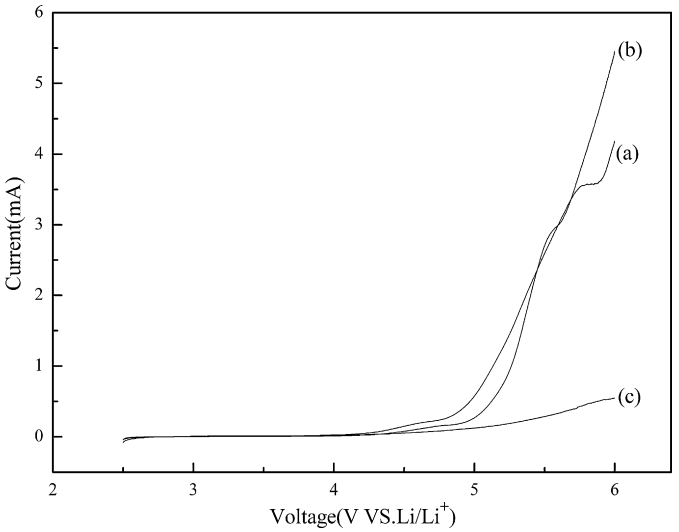

Fig. 8. Linear sweep voltammograms of the gel polymer electrolytes (a) without in situ ceramic fillers, (b) with 3% in situ SiO_2 and (c) with 3% in situ TiO_2.

membrane without in situ ceramic fillers (4.8 V) < in situ SiO_2 (5.0 V) < in situ TiO_2 (5.4 V). From Fig. 8, we can see clearly that the gel polymer electrolyte with in situ TiO_2 shows the best electrochemical stability. A decomposition process, which is associated with electrode/electrolyte, results in the onset of current flow in the high voltage range. And this onset voltage is the upper limit of the electrolyte stability range. There is no electrochemical reaction in the potential range from 3.0 V to 5.4 V in Fig. 8(c). The onset of current flow at 5.4 V is related with the decomposition of the lithium electrode. Upon further increase of the cell voltage, a considerable current began to flow, indicating the onset of electrolyte decomposition process.

The partial swelling of the in situ TiO_2 membrane with a large surface area significantly contributed to the increase in the stability of the electrolyte solution under electrochemical environments, although the ionic conduction occurred mainly through the entrapped liquid electrolyte in the pore structure. Therefore, the swollen phase of the membrane probably includes the complex compounds such as associated VdF–Li^+ groups. This complex formation with lithium ion and VdF groups of PVdF enhances the electrochemical stability of GPEs. The electrochemical stability was also influenced by the large and fully interconnected pores, high porosity, higher specific surface area, uniform morphology of membranes and the AFDs. The oxidation stability of the GPE increased with the decreasing of AFDs. So the gel polymer electrolyte with in situ TiO_2 shows the best electrochemical stability.

The high anodic stability of these polymer electrolytes should render them very suitable for applications in lithium-ion battery.

4. Conclusions

TPU–PVdF based gel polymer electrolytes with and without in situ ceramic fillers (SiO_2 and TiO_2) have been prepared by electrospinning the 9 wt% polymer solution in DMF/acetone (3:1, w/w) at room temperature. The gel polymer electrolytes were prepared by activating the dried electrospun nonwoven films in 1 M $LiClO_4$–EC/PC liquid electrolyte solutions. All of the gel polymer electrolytes have high ionic conductivity and good electrochemical stability >4.6 V versus Li/Li^+. It generally observed that both the ionic conductivity and the mechanical properties are improved after the addition of in situ ceramic fillers. The optimum performance has been observed for the gel polymer electrolyte with in situ TiO_2. It displays the widest electrochemical stability up to 5.4 V versus Li^+/Li at 25 °C. And it has a perfect mechanical stability with high tensile strength (8.7 ± 0.3 MPa) and % elongation at break (110.3 ± 0.2). And its ionic conductivity is as high as 4.8×10^{-3} S cm^{-1} at room temperature. These results suggest that incorporation of in situ generated TiO_2 is more efficient in improving the properties of gel polymer electrolyte for practical application.

Acknowledgements

This work was supported by Hunan Provincial Education Department Youth Project Fundation under contract number 09B101.

References

[1] Y.J. Hwang, K.S. Nahm, T.P. Kumar, A.M. Stephan, J. Membr. Sci. 310 (2008) 349–355.
[2] N. Muniyandi, N. Kalaiselvi, P. Periyasamy, R. Thirunakaran, B.R. Babu, S. Gopukumar, N.G. Renganathan, M. Raghavan, J. Power Sources 96 (2001) 14–19.
[3] Q.Z. Xiao, Z.H. Li, D.S. Gao, H.L. Zhang, J. Membr. Sci. 326 (2009) 260.
[4] P. Raghavan, J.W. Choi, J.H. Ahn, G. Cheruvally, G.S. Chauhana, H.J. Ahn, C. Nah, J. Power Sources 184 (2008) 437–443.
[5] C.R. Yang, Z.D. Jia, Z.C. Guan, L.M. Wang, J. Power Sources 189 (2009) 716.
[6] Z.H. Li, P. Zhang, H.P. Zhang, Y.P. Wu, X.D. Zhou, Electrochem. Commun. 10 (2008) 791.
[7] K. Gao, X. Hu, T. Yi, C. Dai, Electrochim. Acta 52 (2006) 443.
[8] S. Rajendran, M.R. Prabhu, M.U. Rani, J. Power Sources 180 (2008) 880.
[9] M.M. Rao, J.S. Liu, W.S. Li, Y. Liang, Y.H. Liao, L.Z. Zhao, J. Power Sources 189 (2009) 711.
[10] H. Cheng, C.B. Zhu, B. Huang, M. Lu, Y. Yang, Electrochim. Acta 52 (2007) 5789.
[11] H.H. Kuo, W.C. Chen, T.C. Wen, A. Gopalan, J. Power Sources 110 (2002) 27–33.
[12] P. Santhosh, T. Vasudevan, A. Gopalan, K.P. Lee, Mater. Sci. Eng. B 135 (2006) 65.
[13] Y.L. Du, T.C. Wen, Mater. Chem. Phys. 71 (2001) 62.
[14] Z.H. Li, H.P. Zhang, P. Zhang, G.C. Li, Y.P. Wu, X.D. Zhou, J. Membr. Sci. 322 (2008) 416.
[15] P.P. Prosini, P. Villano, M. Carewska, Electrochim. Acta 48 (2002) 227.
[16] P. Zhang, H.P. Zhang, G.C. Li, Z.H. Li, Y.P. Wu, Electrochem. Commun. 10 (2008) 1052.
[17] M.M. Rao, J.S. Liu, W.S. Li, Y.H. Liao, Y. Liang, L.Z. Zhao, J. Solid State Electrochem. 14 (2009) 255.
[18] J.Y. Xi, X.P. Qiu, M.Z. Cui, X.Z. Tang, W.T. Zhu, L.Q. Chen, J. Power Sources 156 (2006) 581.
[19] J.R. Kim, S.W. Choi, S.M. Jo, W.S. Lee, B.C. Kim, Electrochim. Acta 50 (2004) 69.
[20] J.R. Kim, S.W. Choi, S.M. Jo, W.S. Lee, B.C. Kim, J. Electrochem. Soc. 152A (2005) 295.
[21] F. Croce, G.B. Appetacchi, L. Persi, B. Scrosati, Nature (London) 394 (1998) 456.
[22] Y.J. Wang, D. Kim, Electrochim. Acta 52 (2007) 3181–3189.
[23] P. Raghavan, X.H. Zhao, J. Manuel, G.S. Chauhan, J.H. Ahn, H.S. Ryu, H.J. Ahn, K.W. Kim, C.W. Nah, Electrochim. Acta 55 (2010) 1347–1354.
[24] J.R. Kim, S.W. Choi, S.M. Jo, W.S. Lee, B.C. Kim, Electrochim. Acta 50 (2004) 69–75.
[25] X.M. He, Q. Shi, X. Zhou, C.R. Wan, C.Y. Jiang, Electrochim. Acta 51 (2005) 1069–1075.